4-2021

Boundary precedence image inpainting method based on self-organizing maps

Haibo PEN

Quan WANG

Zhaoxia WANG
Singapore Management University, zxwang@smu.edu.sg

Knowledge-Based Systems 216 (2021) 106722

Contents lists available at ScienceDirect

Knowledge-Based Systems

journal homepage: www.elsevier.com/locate/knosys

Boundary precedence image inpainting method based on Self-organizing Maps

Haibo Pen [a], Quan Wang [b], Zhaoxia Wang [c,*]

[a] Key Laboratory of Smart Grid of Ministry of Education, School of Electrical and Information Engineering, Tianjin University, Tianjin, China
[b] Internet FinTech Department, China Banking and Insurance Information Technology Management Company Ltd., Beijing, China
[c] School of Information Systems, Singapore Management University, Singapore

ARTICLE INFO

Article history:
Received 9 August 2020
Received in revised form 18 November 2020
Accepted 21 December 2020
Available online 18 January 2021

Keywords:
Image inpainting
Layer separation
Self-organizing Maps (SOMs)
Boundary precedence (BP)

ABSTRACT

In addition to text data analysis, image analysis is an area that has increasingly gained importance in recent years because more and more image data have spread throughout the internet and real life. As an important segment of image analysis techniques, image restoration has been attracting a lot of researchers' attention. As one of AI methodologies, Self-organizing Maps (SOMs) have been applied to a great number of useful applications. However, it has rarely been applied to the domain of image restoration. In this paper, we propose a novel image restoration method by leveraging the capability of SOMs, and we name it "boundary precedence image inpainting method based on SOMs". In the proposed method, SOMs are used to separate a damaged image into different layers according to the pixel information of the image. Each pixel in the damaged area is considered to be a center of a square area, which is called a waiting-for-inpainting patch. The waiting-for-inpainting patch filling order is calculated by the boundary precedence method in which the information of the separated image layers obtained by SOMs is analyzed and used to calculate the filling order. According to the proposed method, the waiting-for-inpainting patches on the boundaries of the damaged region are restored first and the filling order of this proposed method depends on the precedence values of each waiting-for-inpainting patch. Case studies demonstrate the effectiveness of this proposed method. Both textural and structural information can be nicely repaired by the proposed method.

1. Introduction

The internet is abound with social media that offer useful data and enable people to share information as well [1]. Such web data or information includes numeric data as well as non-numeric data. Non-numeric data take on different forms, such as texts (e.g. internet forums, weblogs, social and micro blogs, wikis, etc.), images (e.g. scanned documents, graphs, charts, photographs, pictures, icons, etc.), videos (moving images), etc. Being able to make sense of non-numeric data, such as text data, is important. Patterns may be hidden within text data such as comments, feedback and critiques, but they do provide useful information. Opinion and sentiment patterns discovered on the internet through text data analysis can be used to characterize an individual's attitude towards issues in their domain of social involvement. In addition to text data analysis, image analysis is an area that has been experiencing a gain in importance due to the significant increase in the use of images and videos over the internet. On top of that, vision is the most advanced human sense among the five senses (i.e., vision, hearing, smell, taste, and touch senses) [2], and the corresponding image analysis and processing technologies, such as image classification, image enhancement, image segmentation, and image reconstruction have been gaining much research attention in the aerospace, medical, energy and almost all other domains. It has successfully led to the development and progress of corresponding fields relevant to image processing [3–6]. Therefore, it is not surprising that images (static or dynamic) play an important role and have become a popular form of data over the internet and real life.

However, from the perspective of both sender and receiver, as an important information carrier for the expression of idea, a critical question is whether the received image data is consistent with the source image. In other words, missing parts of the image information caused by some interference events may lead to difficulty in accurately understanding the sender's idea [7–9]. For example, as one of the most valuable cultural expressions of mankind, mural paintings play an important role for the understanding of ancient societies and civilizations. However, due to

* Corresponding author.
E-mail addresses: penhaibo@tju.edu.cn (H. Pen), zxwang@smu.edu.sg (Z. Wang).
URL: https://www.smu.edu.sg/faculty/profile/161841/WANG-Zhaoxia (Z. Wang).

https://doi.org/10.1016/j.knosys.2020.106722
0950-7051/

the location, environment of the murals and human factor, mural paintings have suffered delamination, efflorescence, cupping, flaking, scratching, falling off, and other damages. It is difficult for modern humans to obtain the whole mural painting information and appreciate its great historical and artistic value [10]. In addition, photographs are the connection to the past and serve as a reminder of significant moments and possess great sentimental values. Even though time has gone by, one can still evoke memories of the past by viewing them. Therefore, missing or damaged image information reconstruction remains an important task. It is of great significance if a method of restoring the integrity of the image can be found [11].

The aim of this paper is to address the problem of image information loss by leveraging self-organizing maps. The main contributions of this paper are threefold as follow:

(I) Main algorithm: We propose a novel image restoration method by leveraging a kind of neural network — Self-organizing Maps (SOMs) to solve the problem of inpainting the missing small-scale information in images.

(II) Restoration model: In the restoration process, the proposed method fully considers the information type included in the damaged image, and applies SOMs to separate a damaged image into multiple different layers according to the pixel information of the image and obtain the best restore order precedence values of the pixels in the damaged area. Then the information of the damaged area will be restored by the patch-based method according to the precedence values, which decides the filling order.

(III) Filling order and search space: The waiting-for-inpainting patch filling order is dependent on precedence values which are computed by the proposed boundary precedence method. In the filling process, the repairability of the damaged patch and the structural information of image are fully considered. As for the search space, multiple separated layers of the damaged image obtained by SOMs reduce the number of search pixels in each layer.

The rest of this paper is organized as follows. Section 2 discusses the research that has been done in this area. Section 3 presents the proposed image inpainting method by describing its layout, principle, procedure, formulation and potentials for addressing image inpainting problems. Section 4 presents the results of the novel proposed method compared with other methods. Finally, Section 5 concludes the paper and suggests further works.

2. Previous works

As an important segment of image analysis techniques, image inpainting or restoration has been attracting more and more researchers' attention since it was introduced by Bertal-mio et al. [12]. Image inpainting is the process of restoring missing or damaged areas in an image [13–16]. Image restoration has been widely practiced since the Renaissance and this includes everything from mere touching up of the images involved to reconstituting entire section of missing or damaged portions of the image. There are generally three categories of methods – Diffusion-based techniques, sparse-based techniques and exemplar-based techniques [17].

Diffusion-based techniques involve propagating linear structures via diffusion based on partial differential equations and variational methods [18]. For instance, a digital image inpainting scheme was firstly proposed by Bertalmio et al. and it is based on higher order Partial Differential Equations (PDE) [12]. PDE scheme diffuses the information of the regions around the damaged regions by leveraging the advantage of thermo diffusion equation. Amrani et al. proposed an inpainting method based on partial differential equations to compress hyperspectral images. They inpaint separately the known data in the spatial and spectral dimensions [19]. Another common diffusion-based approach is the Total Variation (TV) approach. The main idea of the TV method is to imitate the process of human inpainting. It is based on the geometric image model and works remarkably well for inpainting small scale damages [20]. In general, this type of diffusion-based algorithm is suitable for small scale damaged areas without complex texture. However, when inpainting large scale damaged areas, they may tend to produce blurring artifacts.

Exemplar-based methods were proposed for inpainting larger scale damages. Such methods include an essential process that replicates both structure and texture for texture synthesis [21–23]. The texture to be synthesized is learned from similar regions in a texture sample or from the known part of the image [17]. Criminsi et al. made use of the exemplar-based approach to remove large objects from images [21]. They also introduced an exemplar-based inpainting method in which the patches containing the strongest iso-phote is selected to patch first [21]. Ghorai et al. improved Criminisi's exemplar-based inpainting algorithm and made use of probabilistic latent semantic analysis (pLSA) method. They leveraged the context and the histogram similarity measure between the candidate patches and target patches [24]. Liu et al. proposed an exemplar-based model which relies on the global minimization of energy function using the graph cuts algorithm that enforces both structure and texture consistency [25]. Wang et al. combined Criminisi's exemplar-based algorithm together with fast Fourier transform to obtain better and faster matching recovery results [26]. Overall, this kind of exemplar-based algorithm is good at texture and large missing areas. However, the structural discontinuities of the inpainted image may appear when the visual consistency is not considered.

Sparse-based inpainting techniques make use of signal sparse representation to address the inpainting problem [27]. Dong et al. and Jin et al. proposed different methods making use of sparse representations over redundant dictionary and sparse coefficients to address the problem of image inpainting [28,29]. Zhang et al. choose groups which are composed of nonlocal patches with similar structures instead of patches as the basic units of sparse representation in the process of image inpainting [30]. However, sparse representation image inpainting methods may fail to restore the structure when filling large missing regions.

In the meantime, as a technique of imitating human brain thinking processes, neural networks, have received a lot of attention from researchers in various domains such as medicine, biology, economics, engineering science and other fields [31–33]. In the image processing domain, image inpainting methods based on deep learning perform effectively in many situations [34]. However, this type of inpainting algorithm needs lots of images and much training time, which is not suitable for situations in which there is a lack of a large number of training samples. The Self-organizing Maps is a kind of neural networks which is different from other artificial neural networks in the sense that they can automatically recognize patterns by using unsupervised learning.

SOMs have been applied to almost all kinds of scenes in the image processing domain. In the last decade, SOMs have been applied to image compression, image segmentation, feature abstraction and classification of image, and the effectiveness has been demonstrated [35–37]. However, there is a limited number of publications on the application of SOMs to image inpainting. Wang et al. first proposed the idea that employed SOMs to the image inpainting process and obtained good results [38]. They leveraged SOMs to separate the damaged image into several layers, and the damaged pixels which were located at different layers were restored respectively by using an 'onion-peel' filling order. The restored layers were united together to give the final inpainted results [38]. Favorskaya et al. handled the image

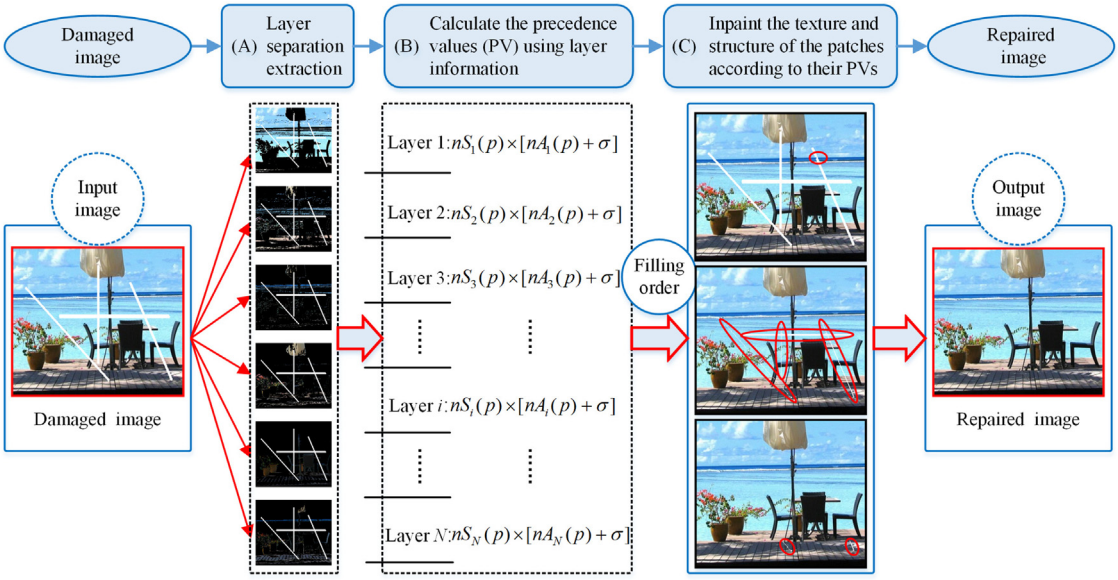

Fig. 1. Layout of the proposed image inpainting method (A) Separate the input damaged image into multiple layers, (B) Calculate the PV of all damaged pixels in each layer, (C) Inpaint the textural and structural information of the damaged area into the corresponding output repaired image.

inpainting problem differently by using four different types of agent: "Agent-operator, Interface Agent, Learning Agent and Inpainitng Agent" and leveraged SOMs for each type of homogenous textures for an image [39].

Whatever kind of inpainting technique the researchers used, in order to realize the connectivity principle of human visual perception [40], filling order is very important [21,40,41]. The default favorite filling order is 'onion-peel', but it has been pointed out that the 'onion-peel' method has shortcomings and tends to produce unexpected artifacts [41]. The best-first filling strategy that depend entirely on the precedence values was found to be better than the 'onion-peel' filling method [21].

3. The proposed inpainting strategy

This paper proposes a boundary precedence image inpainting method based on SOMs. In this section, the layout of the proposed method is given first. Then we describe the three core parts of our algorithm one after another, including layer separation; the precedence value (PV) calculation; and image textural and structural information restoration.

3.1. Layout of the proposed method

The layout of the proposed method is illustrated in Fig. 1. First, the process begins with an input damaged image which lacks scratch information. Next, the damaged image is separated into several layers by the SOMs in the Layer separation Block. Then, using the information of the separated layers, the precedence values (PV) of the patches are calculated in the Calculate the PV Block. Afterwards, as shown by the red circle marks, the patches are inpainted individually according to their PVs. The 'waiting-for-inpainting' patches and the layers are updated after all damaged patches are filled. Finally, when all the damaged pixels have been filled, the repaired image is obtained.

3.2. Layer separation

Traditional clustering analysis has been used to identify inherent structures and classify useful information from large amount of data. However, the users of this technique often have insufficient understanding of the nature of the data and hence

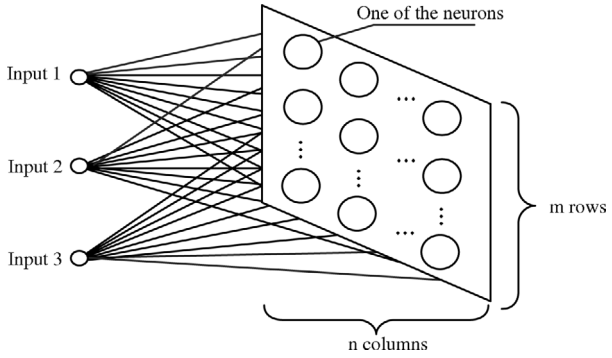

Fig. 2. Architecture of the SOMs.

have difficulties setting the optimal parameters for the clustering method [42]. To overcome the above drawback of the traditional method, this paper proposes image color clustering by using SOMs. Taking advantage of SOMs' powerful ability for clustering, an image can be separated into several layers [38]. The pixels with similar colors in an image will be clustered into the same group, which represents one of the layers of the image.

Choosing RGB space as the image's color space, each pixel's color can be represented by a three dimensional vector. These vectors are also the inputs of the SOMs. The objective of applying SOMs in the proposed method is to divide these vectors into different groups.

The topological structure of the SOMs which has $m\times n$ neurons as shown in Fig. 2 is employed to separate an image into $m \times n$ different layers [38]. Each neuron has 3 inputs, since each pixel is represented by the three color component intensities (Red, Green and Blue). All the useful pixels can be separated into $m \times n$ different groups/layers by SOMs. Takinganimageasanexample, when the parameters m and n are both set as constant 2, the simulation results of the layer separation by SOMs is shown in Fig. 3.

The original image shown in Fig. 3(a) is separated into 4 layers by SOMs as shown in Figs. 3(b)–3(e). The final united result obtained by using the four layers is shown in Fig. 3(f). The separating results is similar to [38]. However, different from [38],

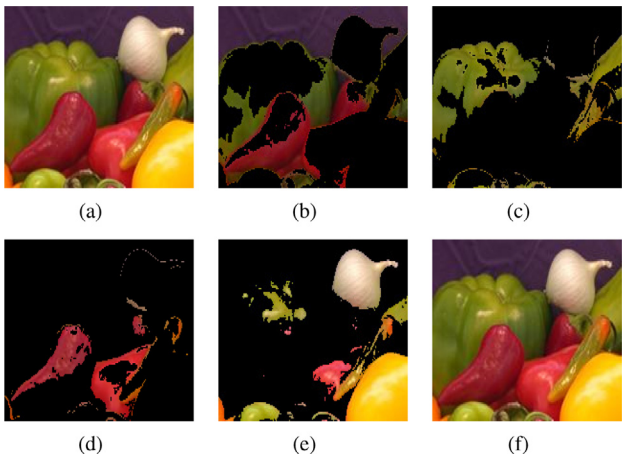

Fig. 3. An example of layer separation by SOMs (a) an example image, which is separated into 4 layers by SOMs, (b) Layer 1 of the example image, (c) Layer 2 of the example image, (d) Layer 3 of the example image, (e) Layer 4 of the example image, (f) the united image of the four layers..

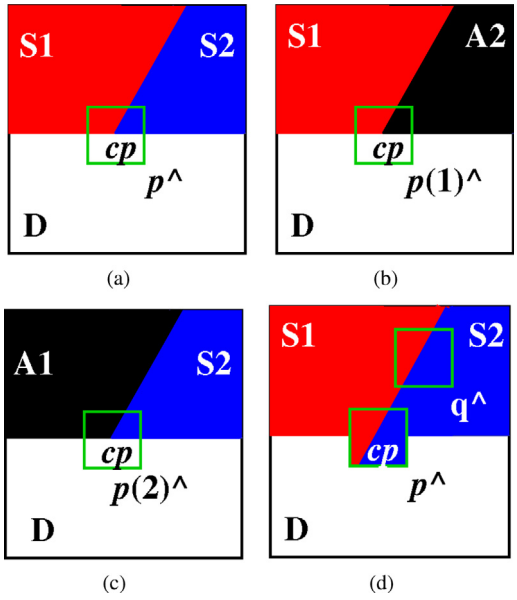

Fig. 4. An example of the process of boundary precedence (a) an example image, in which the target region is marked by the symbol D, (b) Layer 1 of the example image, in which the pixels that do not belong to this layer are marked as black, (c) Layer 2 of the example image, (d) the result of restoring the patch $p^\wedge$ by using patch $q^\wedge$.

the principle of the layer-separating inpainting in this paper is to realize the process of boundary precedence, which will be discussed in Section 3.3.

3.3. Calculating the precedence value (PV) using layer information

As mentioned above, the effect of the image inpainting depends on the filling order. Inpainting process of boundary precedence is determined by using a Boundary Precedence Computing Algorithm (BPCA) which is proposed in this paper. Before describing the mathematical equation of the BPCA, we explain the principle of this algorithm by using a simple two-colored image, which has been separated into two layers as shown in Fig. 4.

Fig. 4(a) shows an example image in which the source region is marked by the symbol S which includes two parts: $S1$ and $S2$. The target region is marked by the symbol D, which is the pure white cp that is the center of patch $p^\wedge$. The example image is separated into 2 layers. Layer 1 of the example image is shown in Fig. 4(b). $p(1)^\wedge$ is the first layer of the patch $p^\wedge$ and the source region only refers to the red region marked by the symbol $S1$ because the primary pixels in blue do not belong to this layer. Therefore, the region in blue in the original image $S2$ has its place taken over by the black region marked by the symbol $A2$ in this layer. Layer 2 of the example image is shown in Fig. 4(c). $p(2)^\wedge$ is the second layer of the patch $p^\wedge$. Similarly, for this layer, the primary pixels in red, $S1$, do not belong to this layer, therefore the region in red in the original image is replaced by the black region marked by $A1$ in this layer. The layer information of $S1$, $A1$, $S2$ and $A2$ are used to calculate the patch priorities to realize the proper filling order of the proposed method. The precedence value $P(p)$ of patch $p^\wedge$ is defined and calculated by the following equation which is the mathematical equation of the proposed BPCA:

$$P(p) = \max\{(nS_1(p)\cdot[nA_1(p)+\sigma]), (nS_2(p)\cdot[nA_2(p)+\sigma])\} \quad (1)$$

where, $nS_1(p)$ and $nS_2(p)$ are the numbers of the source pixels within the patch $p^\wedge$ in Layer 1 and Layer 2, respectively. $nA_1(p)$ and $nA_2(p)$ are the numbers of the source pixels which do not belong to Layer 1 and Layer 2, respectively. There is a delicate balance between $nS_i(p)(i = 1, 2)$ and $nA_i(p)(i = 1, 2)$, and the balance can be adjusted by setting the parameter, σ.

Fig. 4 is a simple illustration that an image is separated into N=2 layers. Generally, a damaged image can be separated into $m \times n = N(N > 2)$ layers by SOMs. The following mathematical expression can be deduced by using Eq. (1):

$$P(p) = \max_{i=1}^{N}\{nS_i(p)\cdot[nA_i(p)+\sigma]\} \quad (2)$$

where, $nS_i(p)$ is the number of the source pixels within the patch $p^\wedge$ in the ith layer. $nA_i(p)$ is the number of the source pixels which do not belong to the ith layer. The parameter, σ is used to adjust the balance between $nS_i(p)$ and $nA_i(p)$. It reflects the proportion of boundary and structural information to the precedence value of the 'waiting-for-inpainting' patch. In this paper, taking the order of magnitude of $nS_i(p)$ and $nA_i(p)$ simultaneously, the default value of σ is set as a constant $\sigma = 0.1$.

When the patch $p^\wedge$ has the highest precedence value, the best-matching patch $q^\wedge$ in the source region is found and is copied into the position occupied by $p^\wedge$, thus achieving partial filling of target region D. As shown in Fig. 4(d), both texture and structure have been propagated inside the target region D.

The priority of a patch is based on the number of the source pixels within the patch $p^\wedge$. Eqs. (1) and (2) show that those patches which are located on the damaged boundary and near to the original undamaged part (i.e. source pixels) have higher precedence values. When all of the boundaries have been restored, the interior part of the target region is then restored step by step.

The BPCA as described in mathematical equation (2) provides the algorithm to realize the proposed inpainting process of boundary precedence.

3.4. Propagating textural and structural information and updating

When the patch $p^\wedge$ with the highest precedence value is obtained, it will be filled with the data extracted from the source region just as shown in Fig. 4(d). Similar to [21], when the patch $p^\wedge$ which has the highest precedence value is obtained, the proposed method will search in the source region to find the most similar patch to the patch $p^\wedge$ by using the following equation:

$$q^\wedge = \min_{q\in D}\{d(p^\wedge, q)\} \quad (3)$$

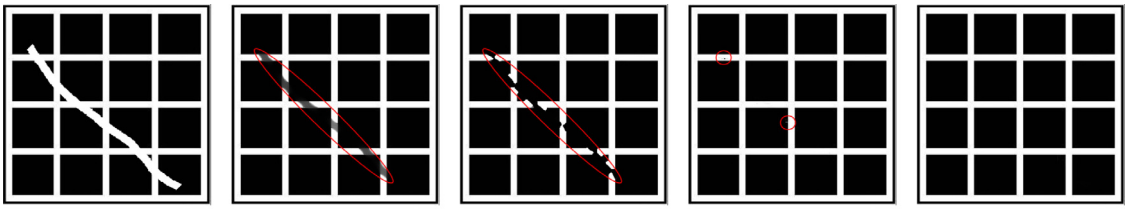

Fig. 5. Case 1: a synthetic image. (a) The damaged image, (b) Inpainting result of TV method, (c) Inpainting result of previous SOMs based method, (d) Inpainting result of exemplar-based method, (e) Inpainting result of novel proposed method.

where, $d(a, b)$ represents the distance between two generic patches a and b. It is obtained as the sum of squared differences between the two patches. The value of each pixel to be replaced, $\{p' \mid p' \in p^{\wedge} \bigcap D\}$, is copied from its corresponding position inside $q^{\wedge}$.

This method fulfills the propagation of the textural as well as the structural information from the source region S to the target region D as shown in Fig. 4(d). After the patches $p^{\wedge}$ have been replaced by new pixel values, the priorities of the unfilled pixels are updated, and then the new $p^{\wedge}$ with the highest PV is calculated according to Eq. (2), and repaired according to Eq. (3). When all the damaged pixels have been filled, the inpainted image is obtained.

4. Results and discussion

In this section, the proposed method is used to inpaint different images which include purely synthetic images as well as full-color photographs. The latter ones are complex in texture and structure. An RGB image can be regarded as a collection of 3-dimension arrays. The value of each pixel according to RGB color component, Red, Green, and Blue are $[x_1, x_2, x_3]$, $x_i \in [0, 255]$, which represents the brightness of the pixel. Correspondingly, a gray image can be regarded as a 2-dimensional array. In all the images, the small size damaged region in the image is the given target region. The default size of the patch $p^{\wedge}$, which is shown in Fig. 4 as the green grid, is set at 3×3 pixels and the parameters of the topological structure of the designed SOMs are set as $N = m \times n = 2$ for this case. The TV method is often selected as a basic reference for inpainting small scale damages and scratches. We compared our proposed method with the TV method, previous SOMs based method, as well as exemplar-based inpainting method. In all the figures of the different cases studied below, (a) is the damaged picture, (b) is the image resulting from using the TV method in [20], (c) is the image resulting from using the previous SOMs based method in [38], (d) is the image resulting from using the exemplar-based method in [24], and (e) is the image resulting from using the method proposed in this paper. It can be seen that (e) is always the best result.

We carried out further experiments by using other parameters of the topological structure of SOMs. The images are separated into fewer than or slightly more than 4 layers, such as $N = 1 \times 3 = 3$, $N = 1 \times 5 = 5$, $N = 2 \times 3 = 6$, $N = 2 \times 4 = 8$, $N = 3 \times 3 = 9$, $N = 3 \times 4 = 12$, and $N = 4 \times 4 = 16$. The experiments demonstrate that separating an image into 3–6 layers is enough to inpaint the damaged image perfectly by using the proposed method.

4.1. Subjective visual evaluation

Fig. 5 shows the results of employing the proposed image inpainting method on a purely synthetic image (Case 1). Fig. 5(a) is a 311×300 pixel synthesized image, which is damaged by drawing a randomly jagged bold line. As shown in Figs. 5(b), (c) and (d), we can still see the traces (highlighted in red ellipses) of the damaged parts after being repaired by the other methods, while the image repaired by our proposed method looks the same as the original one with no traces of the damage parts as shown in Fig. 5(e). Both textures and structures have been automatically propagated into the target region perfectly.

The results on two grayscale images are shown in Fig. 6 (Case 2) and Fig. 7 (Case 3). The image used in Fig. 6 is a 256×256 pixel grayscale photograph, while the one in Fig. 7 has dimensions 512×512. Similar to Case 1, the traces (highlighted in red ellipses) of damaged parts can still be seen in the repaired image that was repaired by the other methods, while no traces of the damaged parts that can be seen in the image repaired by our proposed method.

Two full-color photographs which are prominent in texture and structure were tested on as well, as the fourth and fifth cases, and the results are shown in Figs. 8 (Case 4) and 9 (Case 5). For Case 4, the traces of the damaged regions can still be seen easily as shown in Figs. 8(b), (c) and (d) (highlighted in red ellipses), while the human eye cannot discern any trace of the damaged parts in the images repaired by our proposed method, as shown in Fig. 8(e). Similar to the above Case 1 to Case 4, in Case 5, it is obvious that there are unrepaired regions (marked by red ellipses) in Figs. 9(b), (c) and (d) which are image repaired by the other methods, while the image repaired by the proposed method looks perfectly repaired as shown in Fig. 9(e).

In all of the cases, it can be observed that certain damaged regions of the image, especially the structural information, could not be restored by TV. The results in all of the cases demonstrate the ability of our proposed method to inpaint both texture and structure better than the TV method and the other methods proposed in [20,24,38].

4.2. Quantitative evaluation

In order to further demonstrate the effectiveness of the proposed method, we compare the similarity between the original images and the images repaired by the proposed method and other methods. As one of the most widely applied methods to compute image similarity, the histogram distance metrics proposed by Bhattacharyya are selected as the similarity evaluation method in this paper [43,44]. The similarity, $S(H_1, H_2)$, between the two images is obtained as follows.

$$S(H_1, H_2) = \sqrt{1 - \sum_{i=1}^{N} \frac{\sqrt{H_1(i) \cdot H_2(i)}}{\sqrt{\sum_i H_1(i) \cdot \sum_i H_2(i)}}} \tag{4}$$

where, H_1 and H_2 are the histogram data of two images. In this paper, they are the original image and inpainted image, respectively.

Because the function of image inpainting is to repair the damaged parts, comparing the repaired damaged regions with the original ones will reflect the performance of the image inpainting

Fig. 6. Case 2: a grayscale photograph. (a) The damaged image, (b) Inpainting result of TV method, (c) Inpainting result of previous SOMs based method, (d) Inpainting result of exemplar-based method, (e) Inpainting result of novel proposed method.

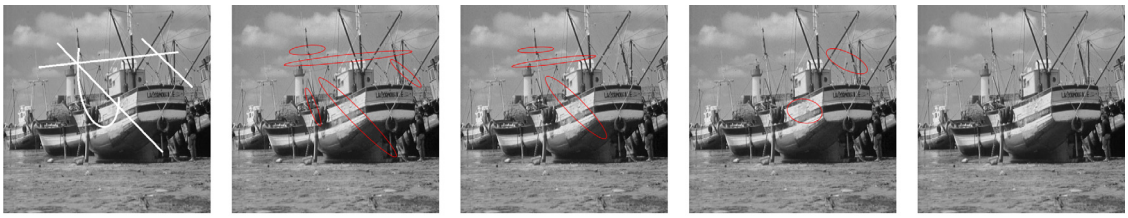

Fig. 7. Case 3: a grayscale photograph of a boat. (a) The damaged image, (b) Inpainting result of TV method, (c) Inpainting result of previous SOMs based method, (d) Inpainting result of exemplar-based method, (e) Inpainting result of novel proposed method.

Fig. 8. Case 4: An image of the Lichtenstein Castle in color. (a) The damaged image, (b) Inpainting result by TV method, (c) Inpainting result of previous SOMs based method, (d) Inpainting result of exemplar-based method, (e) Inpainting result of novel proposed method.

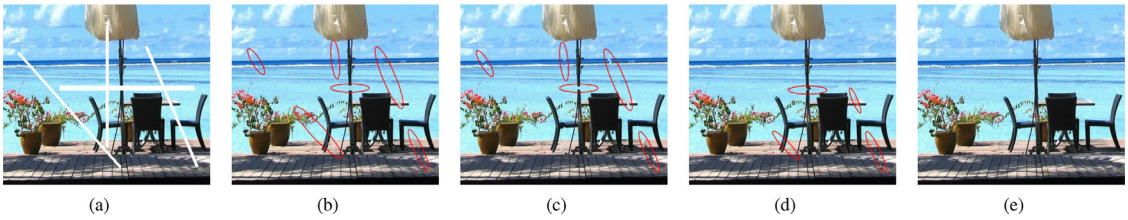

Fig. 9. Case 5: a colorful photograph. (a) The damaged image, (b) Inpainting result by TV method, (c) Inpainting result of previous SOMs based method, (d) Inpainting result of exemplar-based method, (e) Inpainting result of novel proposed method.

methods. So we focus on calculating the similarity function between the images in the damaged regions and the original ones to evaluate the performance of the proposed method.

There are different formats of images, such as grayscale and full-color formats. In order to prove the robustness of the proposed method, different images in different formats had been leveraged as case studies to test the proposed method. In this paper, the restoration performance of the proposed method is tested by comparing the similarity between the initial images and repaired images by using the different images in different formats — the grayscale, RGB and HSV formats.

4.2.1. In grayscale space

When the similarity evaluation is performed in grayscale space, the histograms of the images are quantized into 256 bins in order to represent the color content of the image. According to Eq. (4), the similarity results are obtained as shown in Table 1.

Table 1 shows the similarity between the original image and repaired image obtained based on the grayscale space histogram. For Case 1, a synthetic image — Grid, it is obvious that the proposed method provides a better performance than the TV method, the previous SOMs based method and the exemplar-based method. For example, the similarity is only 0.352 for the repair obtained by the TV method [20], 0.738 by the previous SOMs based method [38] and 0.845 by the exemplar-based method [24], while the similarity is 0.921 for the repair obtained by the proposed method which is higher than that obtained by the other three methods. The average performance for handling different images is far higher (0.862) than in the other three methods (0.657, 0.756 and 0.818). The objective similarity evaluation results are consistent with the subjective visual evaluation in the previous section.

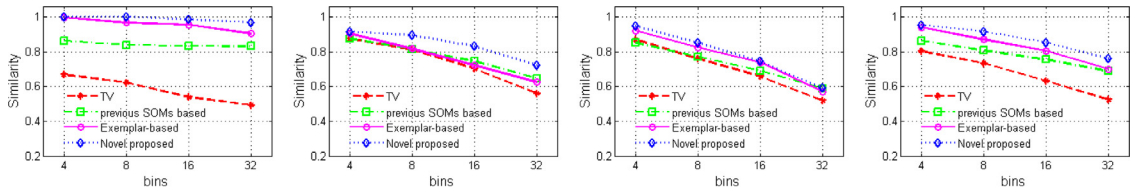

Fig. 10. Similarities for the RGB color space using histogram distance: (a) Case 1: red line with ∗'s, green line with □'s, magenta line with ○'s, blue line with ◇'s represent inpainting image in Fig. 5 using TV, previous SOMs based, Exemplar-based and Novel proposed methods respectively; (b) Case 4: red line with ∗'s, green line with □'s, magenta line with ○'s, blue line with ◇'s represent inpainting image in Fig. 8 using TV, previous SOMs based, Exemplar-based and Novel proposed methods respectively; (c) Case 5: red line with ∗'s, green line with □'s, magenta line with ○'s, blue line with ◇'s represent inpainting image in Fig. 9 using TV, previous SOMs based, Exemplar-based and Novel proposed methods respectively; (d) Average performance: red line with ∗'s, green line with □'s, magenta line with ○'s, blue line with ◇'s represent average value of three color inpainting image using TV, previous SOMs based, Exemplar-based and Novel proposed methods respectively.

Table 1
Image similarities in the grayscale space for different methods.

Case example with image format and image names	Methods			
	TV method	Previous SOMs based method	Exemplar -based method	Novel proposed method
Case 1: a synthetic image-**Grid**	0.352	0.738	0.845	0.921
Case 2: a grayscale image-**Camera**	0.677	0.689	0.719	0.800
Case 3: a grayscale image-**Boat**	0.743	0.709	0.854	0.864
Case 4: a color photograph-**Castle**	0.774	0.834	0.855	0.900
Case 5: a color photograph-**Beach**	0.740	0.810	0.817	0.824
Average performance	0.657	0.756	0.818	0.862

Table 2
Image similarities in the RGB color space for different methods.

Case example with image format and image names	Methods				
	Each layer bins	TV method	Previous SOMs based method	Exemplar -based method	Novel proposed method
Case 1: a synthetic image-**Grid**	4	0.667	0.863	0.997	1.000
	8	0.622	0.838	0.964	1.000
	16	0.537	0.832	0.952	0.983
	32	0.492	0.838	0.903	0.967
Case 4: a color photograph **-Castle**	4	0.873	0.874	0.902	0.915
	8	0.811	0.814	0.816	0.892
	16	0.700	0.743	0.720	0.831
	32	0.559	0.645	0.623	0.719
Case 5: a color photograph **-Beach**	4	0.868	0.849	0.920	0.946
	8	0.759	0.771	0.824	0.850
	16	0.657	0.689	0.737	0.745
	32	0.517	0.587	0.570	0.590
Average performance	4	0.803	0.862	0.940	0.954
	8	0.731	0.808	0.868	0.914
	16	0.631	0.755	0.803	0.853
	32	0.523	0.690	0.699	0.759

4.2.2. In RGB color space

When the similarity evaluation is performed in RGB color space, R, G and B have the same range of values. Hence, for the three full-color images in the previous experiment, they are quantized into the same levels. The objective similarity evaluation results of different images are shown in Fig. 10 and Table 2.

Fig. 10 compares the performance of the proposed method by selecting different parameter bins. The x-axis of Fig. 10 denotes the x^3 color histogram bins and the y-axis denotes the similarities. As shown in Fig. 10, the performance of our current proposed method is vastly better than the other methods compared in this paper. Especially when selecting a large number of color histogram bins, as shown in Fig. 10, it is much more obvious that the performance of our current proposed method is better than that of the other methods. The detailed results are also shown in Table 2. The RGB color space results are also consistent with the subjective visual evaluation of Section 4.1.

Table 3
Image similarities for the HSV color space with different methods.

Case example with image format and image names	Methods			
	TV method	Previous SOMs based method	Exemplar -based method	Novel proposed method
Case 1: a synthetic image-**Grid**	0.677	0.863	0.997	1.000
Case 4: a color photograph-**Castle**	0.787	0.830	0.809	0.910
Case 5: a color photograph-**Beach**	0.792	0.820	0.807	0.850
Average performance	0.752	0.838	0.871	0.920

4.2.3. In HSV color space

When the similarity evaluation is performed in HSV color space, hue (H) component is more important than the saturation (S) and the value (V) components [45]. Hence, assigning more weights to hue (H) than to the other components is reasonable [46]. Therefore, according to [46], this research selects the number of bin levels to be in the ratio of 4:2:2 for the three components, respectively. The similarity results obtained are shown in Table 3.

From Table 3, it can be seen that the performance of this newly proposed method is better than the TV method, the previous SOMs based method and the exemplar-based method. The HSV color space based evaluation is consistent with the other space evaluations. This result also demonstrates the effectiveness and robustness of the proposed method and it can apply to any format of images.

4.2.4. Other quantitative evaluation indices

In order to further demonstrate the image inpainting performance of the proposed method, we further compare our proposed method with the other existing image inpainting methods using quantitative evaluation indices. The four most widely applied evaluation indices are used to compute image similarity, which including Peak Signal to Noise Ratio (PSNR)(dB) [47], FSIM [48],

Table 4
Different quantitative indices of image similarities with different methods.

Evaluation index	Methods			
	TV method	Previous SOMs based method	Exemplar -based method	Novel proposed method
PSNR (dB)	32.7674	30.8090	35.7267	40.2221
FSIM	0.9860	0.9849	0.9874	0.9907
SR_SIM	0.9820	0.9698	0.9918	0.9939
VSI	0.9949	0.9945	0.9954	0.9970

SR_SIM [49], and VSI [50]. In the last three image quantitative evaluation indices mentioned above, the output values fall in the interval (0,1] and it equals 1 when two images are exactly the same. In the meantime, considering that the scratch damaged area is too small to be representative, we select the average value of each index of the damaged area of all the repaired images. The corresponding values of these measures for different methods are shown in Table 4.

From Table 4, it can be seen that the performance of this newly proposed method is also better than the TV method, the previous SOMs based method and the exemplar-based method. The mean PSNR FSIM, SR_SIM, VSI of 40.2221, 0.9907, 0.9939, 0.9970 by the proposed method is much higher than that of the other three approaches. The results of four kinds of similarity comparison methods are also consistent with the above subjective and different color space quantitative visual evaluation. These results further demonstrate the effectiveness and robustness of the proposed method.

5. Conclusion and future works

We leverage the capability of the SOMs and combine it with our new design to propose the boundary precedence image inpainting method. The proposed method takes advantage of the SOMs' ability of unsupervised learning to separate an image into different layers according to the pixel information of an image. The boundary precedence image inpainting process presented in the proposed method is used to calculate the precedence of the waiting-for-inpainting patch according to the layer information obtained by the SOMs to restore the damaged images. The effectiveness as well as the merits of our proposed method is demonstrated by case studies compared with other methods.

More and more image data have spread throughout the internet and real life. Despite significant progress, image analysis and processing are still finding their own voice as inter-disciplinary fields. On the one hand, we look forward to continuing investigation, with the hope to further enhance the intelligent approaches for image processing, which will support higher quality social media applications. On the other hand, the proposed method can be applied to actual scenes such as architecture, mural painting, automatic driving and so on, which shows greater application values.

CRediT authorship contribution statement

Haibo Pen: Investigation, Data curation, Formal analysis, Visualization, Writing - review & editing, Validation. **Quan Wang:** Investigation, Data curation, Software, Writing- original draft. **Zhaoxia Wang:** Conceptualization, Methodology, Visualization, Software, Data curation, Supervision, Writing - original draft, Writing - review & editing.

Declaration of competing interest

The authors declare that they have no known competing financial interests or personal relationships that could have appeared to influence the work reported in this paper.

Acknowledgments

The authors would like to thank the other team members from the Department of Social and Cognitive Computing, Institute of High Performance Computing (IHPC), Agency for Science, Technology and Research (A*STAR), Singapore. Especially, the authors would like to express their special thanks to Senior Scientist, Dr. Ho Seng Beng, for his comments, revisions and proofreading of this paper.

This paper is supported by the China Postdoctoral Science Foundation (2019M651037) and Natural Science Foundation of Tianjin, China (19JCQNJC06000).

References

[1] C. Zuheros, S. Tabik, A. Valdivia, E. Martinez-Camara, F. Herrera, Deep recurrent neural network for geographical entities disambiguation on social media data, Knowl.-Based Syst. 173 (2019) 117–127.
[2] F. Hutmacher, Why is there so much more research on vision than on any other sensory modality? Front. Psychol. 10 (2019) 2246.
[3] E. Kalinicheva, D. Ienco, J. Sublime, M. Trocan, Unsupervised change detection analysis in satellite image time series using deep learning combined with graph-based approaches, IEEE J. Sel. Top. Appl. Earth Obs. Remote Sens. 13 (2020) 1450–1466.
[4] D. Połap, M. Woźniak, Bacteria shape classification by the use of region covariance and Convolutional Neural Network, in: 2019 International Joint Conference on Neural Networks, IJCNN, 2019, pp. 1–7.
[5] W. Wei, B. Zhou, D. Połap, M. Woźniak, A regional adaptive variational PDE model for computed tomography image reconstruction, Pattern Recognit. 92 (2019) 64–81.
[6] Y. Tang, C.-W. Ten, C. Wang, G. Parker, Extraction of energy information from analog meters using image processing, IEEE Trans. Smart Grid 6 (4) (2015) 2032–2040.
[7] Y. Song, J. Zhang, L. Gong, S. He, L. Bao, J. Pan, Q. Yang, M.-H. Yang, Joint face hallucination and deblurring via structure generation and detail enhancement, Int. J. Comput. Vis. 127 (2019) 785–800.
[8] C. Qing, Y. Qiangqiang, M.K.-P. Ng, S. Huanfeng, Z. Liangpei, Missing data reconstruction for remote sensing images with weighted low-rank tensor model, IEEE Access 7 (2019) 142339–142352.
[9] X. Chai, G. Tang, S. Wang, R. Peng, J. Li, Deep learning for regularly missing data reconstruction, IEEE Trans. Geosci. Remote Sens. 58 (6) (2020) 4406–4423.
[10] J. Cao, Y. Li, Q. Zhang, H. Cui, Restoration of an ancient temple mural by a local search algorithm of an adaptive sample block, Heritage ence 7 (1) (2019) 1–14.
[11] Z. Wang, H. Pen, T. Yang, Q. Wang, Structure-priority image restoration through genetic algorithm optimization, IEEE Access 8 (2020) 90698–90708.
[12] M. Bertalmio, G. Sapiro, V. Caselles, C. Ballester, Image inpainting, in: Proceedings of the 27th Annual Conference on Computer Graphics and Interactive Techniques, 2000, pp. 417–424.
[13] Y. Fu, A. Lam, I. Sato, Y. Sato, Adaptive spatial-spectral dictionary learning for hyperspectral image restoration, Int. J. Comput. Vis. 122 (2017) 228–245.
[14] D. Ding, S. Ram, J.J. Rodríguez, Image inpainting using nonlocal texture matching and nonlinear filtering, IEEE Trans. Image Process. 28 (4) (2019) 1705–1719.
[15] Z. Shen, W. Lai, T. Xu, J. Kautz, M.-H. Yang, Exploiting semantics for face image deblurring, Int. J. Comput. Vis. 128 (2020) 1829–1846.
[16] N. Wang, S. Ma, J. Li, Y. Zhang, L. Zhang, Multistage attention network for image inpainting, Pattern Recognit. 106 (2020) 107448.
[17] C. Guillemot, O.L. Meur, Image inpainting: Overview and recent advances, IEEE Signal Process. Mag. 31 (1) (2014) 127–144.
[18] S. Li, X. Yang, Novel image inpainting algorithm based on adaptive fourth-order partial differential equation, IET Image Process. 11 (10) (2017) 870–879.
[19] Naoufal Amrani, Joan Serra-Sagristà, Pascal Peter, Joachim Weickert, Diffusion-based inpainting for coding remote-sensing data, IEEE Geosci. Remote Sens. Lett. 14 (8) (2017) 1203–1207.

[20] J. Aujol, Some first-order algorithms for total variation based image restoration, J. Math. Imaging Vision 34 (3) (2009) 307–327.
[21] A. Criminisi, P. Perez, K. Toyama, Region filling and object removal by exemplar-based image inpainting, IEEE Trans. Image Process. 13 (9) (2004) 1200–1212.
[22] A.S. Hareesh, V. Chandrasekaran, Exemplar-based color image inpainting: a fractional gradient function approach, Pattern Anal. Appl. 17 (2) (2014) 389–399.
[23] H. Liu, X. Bi, G. Lu, W. Wang, Exemplar-based image inpainting with multi-resolution information and the graph cut technique, IEEE Access 7 (2019) 101641–101657.
[24] M. Ghorai, B. Chanda, An image inpainting method using pLSA-based search space estimation, Mach. Vis. Appl. 26 (1) (2015) 69–87.
[25] Y. Liu, V. Caselles, Exemplar-based image inpainting using multiscale graph cuts, IEEE Trans. Image Process. 22 (5) (2013) 1699–1711.
[26] H. Wang, J. Li, R. Liang, X. Li, Exemplar-based image inpainting using structure consistent patch matching, Neurocomputing 269 (2017) 90–96.
[27] J. Mairal, M. Elad, G. Sapiro, Sparse representation for color image restoration, IEEE Trans. Image Process. 17 (1) (2008) 53–69.
[28] W. Dong, G. Shi, Y. Ma, X. Li, Image restoration via simultaneous sparse coding: Where structured sparsity meets Gaussian scale mixture, Int. J. Comput. Vis. 114 (2015) 217–232.
[29] Z. Gao, L. Ding, Q. Xiong, Z. Gong, C. Xiong, Image compressive sensing reconstruction based on z-score standardized group sparse representation, IEEE Access 7 (2019) 90640–90651.
[30] J. Zhang, D. Zhao, W. Gao, Group-based sparse representation for image restoration, IEEE Trans. Image Process. 23 (8) (2014) 3336–3351.
[31] P. Melin, J.C. Monica, D. Sanchez, O. Castillo, Analysis of spatial spread relationships of coronavirus (COVID-19) pandemic in the world using self organizing maps, Chaos Solitons Fractals 138 (2020) 109917.
[32] T. Liu, W. Wu, Y. Zhu, W. Tong, Predicting taxi demands via an attention-based convolutional recurrent neural network, Knowl.-Based Syst. 206 (2020) 106294.
[33] R.M. Luque-Baena, E. López-Rubio, E. Domínguez, E.J. Palomo, J.M. Jerez, A self-organizing map to improve vehicle detection in flow monitoring systems, Soft Comput. 19 (2015) 2499–2509.
[34] Z. Jin, M.Z. Iqbal, D. Bobkov, W. Zou, E. Steinbach, A flexible deep CNN framework for image restoration, IEEE Trans. Multimed. 22 (4) (2020) 1055–1068.
[35] Z. Huang, X. Zhang, L. Chen, Y. Zhu, F. An, H. Wang, S. Feng, A hardware-efficient vector quantizer based on self-organizing map for high-speed image compression, Appl. Sci. 7 (2017) 1106.
[36] E. Aghajari, G.D. Chandrashekhar, Self-organizing map based extended fuzzy C-means (SEEFC) algorithm for image segmentation, Appl. Soft Comput. 54 (2017) 347–363.
[37] C.S. Wicramasinghe, K. Amarasinghe, M. Manic, Deep self-organizing maps for unsupervised image classification, IEEE Trans. Ind. Inf. 15 (11) (2019) 5837–5845.
[38] Q. Wang, Z. Wang, C.S. Chang, T. Yang, Multilayer image inpainting approach based on neural networks, in: 2009 5th International Conference on Natural Computation, vol. 3, 2009, pp. 459–462.
[39] M. Favorskaya, L.C. Jain, A. Bolgov, Image inpainting based on self-organizing maps by using multi-agent implementation, Procedia Comput. Sci. 35 (2014) 861–870.
[40] T.F. Chan, J. Shen, Nontexture inpainting by curvature-driven diffusions, J. Vis. Commun. Image Represent. 12 (4) (2001) 436–449.
[41] G. Peyre, Texture synthesis with grouplets, IEEE Trans. Pattern Anal. Mach. Intell. 32 (4) (2010) 733–746.
[42] D. Jiang, C. Tang, A. Zhang, Cluster analysis for gene expression data: A survey, IEEE Trans. Knowl. Data Eng. 16 (11) (2004) 1370–1386.
[43] A. Bhattachayya, On a measure of divergence between two statistical population defined by their population distributions, Bull. Calcutta Math. Soc. 35 (1943) 99–109.
[44] J. Ning, L. Zhang, D. Zhang, C. Wu, Interactive image segmentation by maximal similarity based region merging, Pattern Recognit. 43 (2) (2010) 445–456.
[45] B.S. Anami, S.S. Nandyal, A. Govardhan, Color and edge histograms based medicinal plants' image retrieval, Int. J. Image Graph. Signal Process. 4 (8) (2012) 24.
[46] N. El-Bendary, E. El Hariri, A.E. Hassanien, A. Badr, Using machine learning techniques for evaluating tomato ripeness, Expert Syst. Appl. 42 (4) (2015) 1892–1905.
[47] H.R. Sheikh, M.F. Sabir, A.C. Bovik, A statistical evaluation of recent full reference image quality assessment algorithms, IEEE Trans. Image Process. 15 (11) (2006) 3440–3451.
[48] L. Zhang, L. Zhang, X. Mou, D. Zhang, FSIM: a feature similarity index for image quality assessment, IEEE Trans. Image Process. 20 (8) (2011) 2378–2386.
[49] L. Zhang, H. Li, SR-SIM: A fast and high performance IQA index based on spectral residual, in: 2012 19th IEEE International Conference on Image Processing, IEEE, 2012, pp. 1473–1476.
[50] L. Zhang, Y. Shen, H. Li, VSI: A visual saliency-induced index for perceptual image quality assessment, IEEE Trans. Image Process. 23 (10) (2014) 4270–4281.